Journal of Innovative Technology, Vol. 4, No. 1, pp. 39-44, March 2022
http://doi.org/10.29424/JIT.202203_4(1).0007

Simulation Studies Analyzing the Hydrodynamic Parameters of Deforming -Non-Newtonian Droplets Settling in Newtonian Fluid

Anjani Ravi Kiran Gollakota [1 *]

ABSTRACT

Non-Newtonian multiphase flows are almost ubiquitous in chemical, biochemical, petroleum and polymer processing industries. Many chemical and processing industries are plagued by bubbles, and many polymeric solutions exhibit non-Newtonian rheological properties. A level set method is used in this study to analyze the rise and deformation of droplets in power-law, and Carreau model non-Newtonian fluid. This simulation is compared to previously published numerical and experimental data to show that the moving droplet interface is viable. The computational geometries used in these comparisons are the same as those reported in the respective literatures. There is good agreement between the current droplet deformation properties and those found in the literature. Computing fluid dynamics-based solver COMSOL Multiphysics 4.3 is used to explore the settling and deformation characteristics of spherical and spheroidal (oblate and prolate) droplets in stagnant air. A two-phase flow system is considered in which the continuous phase is Newtonian medium (air) and the dispersed droplet phase is considered to be both Newtonian fluids (water), Carreau fluid (Emkarox) and the power law fluid (n -0.4). Volume fraction images of spherical and spheroid droplets reveal substantial distortion in the early stages, which gradually decreases as the droplet approaches the channel's bottom. The drag coefficient of a moving droplet is calculated over time to comprehend non-Newtonian droplet settling velocity.

Keywords: Carreau fluid, Power-law fluid, deformation, droplet, drag coefficient

1. INTRODUCTION

Droplet–based microfluidics has recently found applications in lab–on–a–chip, chemical, biological, and nanomaterial creation. An interesting physical phenomenon occurs when droplets interact with solid surfaces in a variety of technical applications such as spray cooling, fire suppression, drop coating for solution-processed solar cells, droplet-based microfluidics, and spray cooling of conductive substrates. Non-Newtonian fluids are just as significant as Newtonian fluids in the design and operation of chemical and biochemical fermentation reactors Chabbra (2006), and Chabbra and Richardson (2008) stress. Taylor and Acrivos, (1964) studied the deformation of non-buoyant slender droplet embedded in the simple extensional flow of a Newtonian liquid and found that the droplet attains a parabolic shape with pointed ends. Acharya et al. (1977, 1978) studied the deformation and drag of the droplet in non-Newtonian liquids at a low Reynolds number. They observed that the bubbles were tear-shaped at a very small Reynolds number and with the increase in Reynolds number the bubble shape tends to be spherical, oblate, and finally spherical capped. Further Acharya et al. (1978) developed a relation between the drag coefficient and Reynolds number in creeping flow regime as a function of power-law or Ostwald de waale fluids. Rust and Manga (2002) studied the effects of bubble deformation on the viscosity of dilute suspensions to bridge the gap between high and low capillary limits and to determine the viscosity of low Reynolds number dilute surfactant-free bubble suspensions where the relative viscosity is sensitive to the changes in shear rate. Garner and Hammerton, (1954) said that the distortion and oscillation of the drop will tend to change the drag coefficient which will make the terminal velocity decreases over the rigid sphere of equal volume. Mohan et al. (1972) reported the terminal velocity of chlorobenzene, nitrobenzene, dibromomethane, and orthonitrotoluene droplets in polymer solutions such as PAA, CMC, PEO. The study reported that small size droplet remains spherical but with the increase in diameter, the drop changes into an oblate spheroidal shape and further increases the diameter of the droplet, the shape further deforms to prolate and finally distortion of the droplet takes place. The addition of the polymer to the continuous phase may increase the surface tension; thus, the droplet remains spherical and the terminal velocity of the smaller drops is reduced whereas the terminal velocity of the larger ones remains the same. Dong et al. (2010) experimentally studied the rise and deformation of a single bubble in ionic liquids by injecting bubbles through orifices of different diameters. Their bubble sizes and aspect ratios are not close to the data that is available in the literature; hence they have developed a correlation for the terminal velocity by adjusting the parameters as a function of Reynolds number and the aspect ratio in addition to a new dimensionless number as a function of Eötvös number. Zhang et al. (2010) studied experimentally and numerically the motion and deformation of a bubble freely rising

Manuscript received March 7, 2022; revised March 22, 2022; accepted March 22, 2022.
[1*] Assistant Professor (corresponding author), Department of Safety, Health and Environmental Engineering, National Yunlin University of Science and Technology, Taiwan (ROC). (email: gollakota.iitg@gmail.com)

through shear thinning Carreau model fluid by using level set method. They observed that for shear thinning non-Newtonian liquids, the power-law index n, has an influence on the bubble rise motion and its deformation. The viscosity around the bubble decreases as n decreases as a result the bubble still rises easily. Kennedy et al. (1994) studied the motion and deformation of the liquid drops and the rheology of dilute emulsions in simple shear flow at low Reynolds numbers. The drop shape is predicted to be perfectly spherical when the capillary number is zero. As the Capillary number has increased the drop elongates and resembles a prolate ellipsoid which agrees with Taylor's small deformation theory where Ca is small and λ =1. A considerable amount of work has been reported on the rise and fall of liquid drops in Newtonian media and the solid sphere falling in a rectangular chamber through both Newtonian and non-Newtonian fluids. However, very little is known about the shape and deformation of the non-Newtonian power law and Carreau fluid droplets of different shapes like sphere, prolate spheroid, and oblate spheroid falling in the Newtonian domains. Thus, the aim of this work is to report numerical results on settling and deformation phenomena of spherical and spheroidal non-Newtonian droplets in a Newtonian medium.

2. PROBLEM STATEMENT AND MATHEMATICAL DESCRIPTION

Droplets of spherical, oblate, and prolate shape are placed in an air-filled chamber at room temperature to analyze their deformation characteristics. Emkarox and CMC were the power law and Carreau model fluids, while air is considered as the Newtonian medium and the summary of the fluid properties were detailed in Table 1. Consider a chamber of width equal to 0.1 times the droplet's width. At a height of 18.5" from the channel's apex, the droplets fall freely, as depicted in Fig. 1**.** The continuous phase is held at a steady state throughout the study, while the deforming medium is held at a transient steady state. The governing continuity and momentum equations of both the phases are as follows:

Table 1 Properties of Continuous and discontinuous phases

S. No	Material	ρ (kg/m^3)	n	λ(s)	μ_0 (kg/m.s)	μ_∞ (kg/m.s)	Simulation Time
1	**Newtonian**						
	Air	1.2	-	-	-	-	0 - 2 Sec
	Water	1000	-	-	-	-	0 – 2 Sec
2	**Carreau Model**						
	Emkarox	970	0.5	1.58	8920	0	0 – 2 Sec
3	**Power Law**						
	n = 0.4	398.107	0.4	-	-	-	0 – 2 Sec

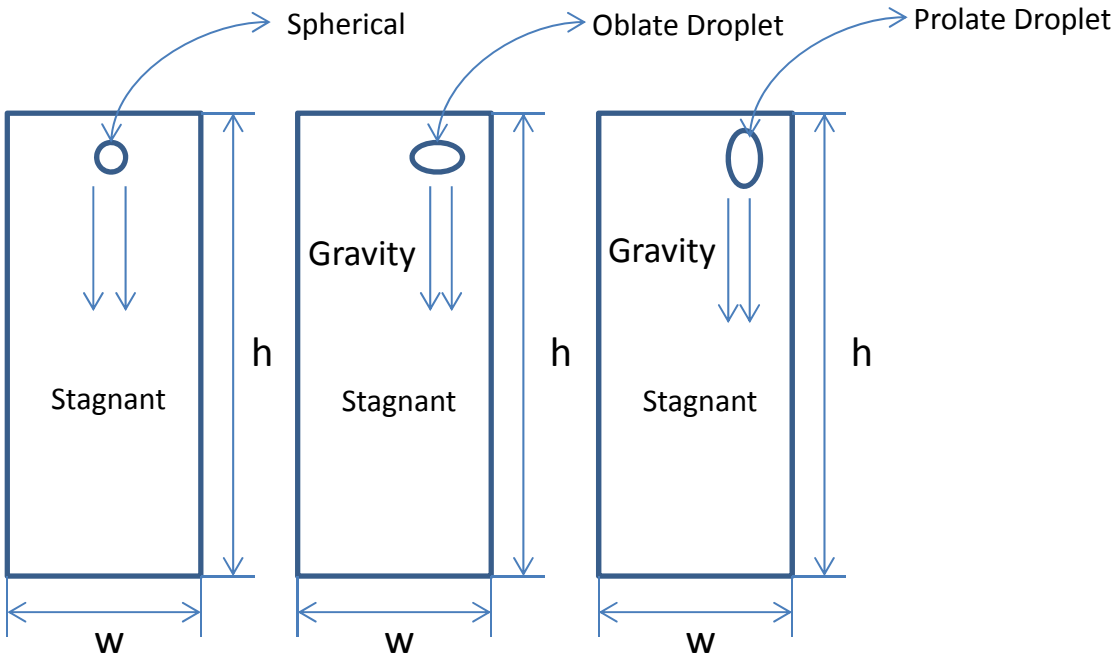

Fig. 1 (a) Computational domain for the spherical droplet in the stagnant air medium, (b) Oblate spheroid droplet in the stagnant air medium, (c) Prolate spheroid droplet in the stagnant air medium

Table 2 Properties of Continuous and discontinuous phases used for validation with Ismail, (2007)

S.No	Material	ρ (kg/m^3)	μ (dynamic viscosity kg/m.s)
1	Oil	880	0.0168
2	Water	997	1.04 x 10^{-3}

Continuity equation:

$$\nabla \cdot V = 0$$

Momentum Equation:

$$\rho\left[\left(V \cdot \nabla\right)V\right] = -\nabla P + \nabla \cdot \tau$$

Extra stress tensor can be written as:

$$\tau = 2\eta\varepsilon$$

Where ρ and η are the density and viscosity of the fluid respectively. Furthermore, the viscosity equation for a power-law fluid can be written as : $\mu = m\left(\frac{I_2}{2}\right)^{(n-1)/2}$ where *m* and *n* are characteristics of a power-law fluid, referred to as power-law consistency index and power-law behavior index, respectively. The rate of deformation tensor (ε) and second invariant of the rate of deformation tensor (I_2) are related to velocity components and their derivatives (see Bird et al., 1960). The Carreau model fluid viscosity can be written as.

Carreau model fluid properties :

$$\frac{\mu_l - \mu_\infty}{\left(\mu_0 - \mu_\infty\right)} = \left[1 + \frac{I_2\lambda^2}{2}\right]^{\left(\frac{n-1}{2}\right)}$$

Where μ_1 is the dynamic viscosity of the fluid, μ_∞ is the infinite shear rate viscosity, μ_0 is the zero shear rate viscosity, λ model parameter, and n flow behavior index.

3. NUMERICAL METHODOLOGY

Using Comsol Multiphysics 4.3, the governing equations and the aforementioned boundary conditions were solved. For each simulation, it takes about 25-30 minutes to run with the fine meshing in order to achieve good convergence and accurate results for the smallest and largest elements of 0.28m, 0.04, and 1.1, respectively. A 0.1-second time step was used to simulate the drop reaching the channel's bottom surface in the (0 – 2 sec) time range. To approximate pressure values, the Lagrange P2P1 technique is utilized to handle velocity-pressure coupling. Dispersed phase properties, such as those of the Carreau model drops and the power-law fluids, will vary depending on fluid characteristics, therefore inputs are set to maintain a constant density and viscosity for the continuous phase. The relative tolerance criterion is set to 10^{-2}, because COMSOL attempts to solve symmetric and non-symmetric systems using the PARDISO solver but fails to achieve the appropriate level of convergence. Different time increments were used to run the simulations. A time-dependent solver is utilized in this study to forecast the drop's velocity and deformation at 0.1 seconds inside the channel, rather than the drop's location within the channel. The domain was selected in such a way to avoid the shear effects as the initial attempt in solving the hydrodynamic properties. Hence fine mesh with 15000 node points was selected to solve the equation and run the simulations.

4. RESULTS AND DISCUSSION

4.1 Validation using COMSOL

Numerical solutions must be validated with existing experimental and/or numerical results to ensure their reliability and accuracy. The container's height and width are chosen to match the study of Ismail (2007) specifications exactly. This study with submerged oil bubbles rising in water that is heavier and immersed with the oil layer on top of the container was used as a first validation case for our method. Table 2 lists the fluid properties used in the comparison case simulation. The scattered phase moves in a continuous phase by buoyancy force when there is a density difference, but no external driving force is provided here. Vertical walls are provided a wetted wall parameter so that fluid interfaces can travel along them, while the top and bottom containers are left without slip conditions. Figure 2 shows the modeling results in good agreement with the experimental results of Ismail (2007). Using this method, we may analyze the deformation of droplets without having them disperse in a stationary environment.

4.2 Volume fraction contours

Volume fractions of spherical, oblate, and prolate power-law and Carreau model droplets that settle in stagnant air are seen in Fig. 3 as a function of time. The droplet moves primarily as a result of the density differential between the scattered and continuous phases, as well as the downward pull of gravity. Due to the fact that surface tension tends to reduce surface area, a droplet with radius R = 0.5 m initially has a perfectly spherical shape, at t=0, i.e., initial velocity. The droplets are allowed to descend slowly as a function of time until they reach the bottom of the channel. As the droplets are descending initially there observed no significant deformation till t= 0.5 sec and a small tail has appeared at t=1.0 sec for both power-law and Carreau model droplets of prolate and oblate shaped droplets. This may be due to the fact that increasing the volume of the droplet under shear thinning effects may lead to the formation of the tail (Gollakota & Kishore, 2017). In the case of the spherical droplets the deformation is quite rapid initiated at t=0.5 sec with a bell-shaped structure with a tailed extension which is the same with the case

of Carreau model droplets. Whereas, the power-law droplet possesses oblate extension just with a small extension due to the viscosity. Similar deformations were continued till the droplets of different shapes in both power law and Carreau models were reported till they reach the bottom of the surface. The spherical droplet at t=1.5 sec for power law and Carreau model fluids were completely deformed. In conclusion, it is understood that the drop deformation occurs under the influence of the viscous forces of the surrounding liquid, external disturbances created due to the wall effects, and the dimensionless parameters called Reynolds number, weber number, and Bond number etc.

4.3 Pressure Distribution

The physics underlying the pressure distribution of the droplets is more generally addressed by examining the air and water systems. The only reason for the drop's mechanical stability is due to the surface forces between the fluid and the drop contact. When surface tension acts alone, it succeeds in molding the drop into a shape with a low surface to volume ratio. The net inward pull of the molecules deeper within the drop increases the surface tension of the liquid, increasing the pressure within the drop and above the prevailing continuous phase outside the drop. The current system demonstrates that the water drop is moving with a terminal velocity, implying that the drop is only being supported against gravity by the vertical component of the pressure forces and the surface shear stresses caused by apparently upward rushing air. Similarly, there should be the same vertical pressure gradient should exist within the drop of exactly the sort found in any mass of fluid (air) at rest in a gravitational field. Spilhaus (1948) show that for large drops larger than 0.05cm, the difference in hydrostatic pressure between the top and bottom of the drop becomes quite important in controlling the drop shape. Figures 7-8 depict the pressure distribution around spherical and spheroidal droplets in the continuous phase and different dispersed phases, namely the Carreau model droplet (Emkarox) (Fig. 4) and the power law droplet.

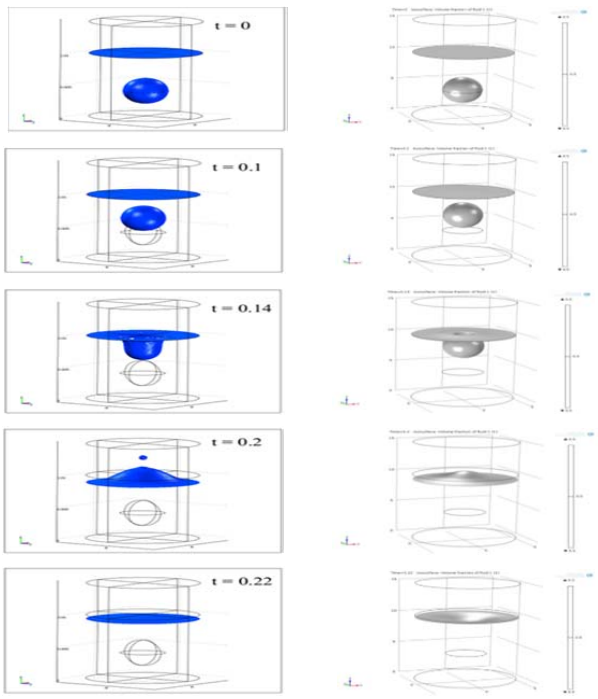

Fig. 2 Comparison of Volume fraction images of Oil bubble rising in water observed in Ismail (2007) and the present predicti ons

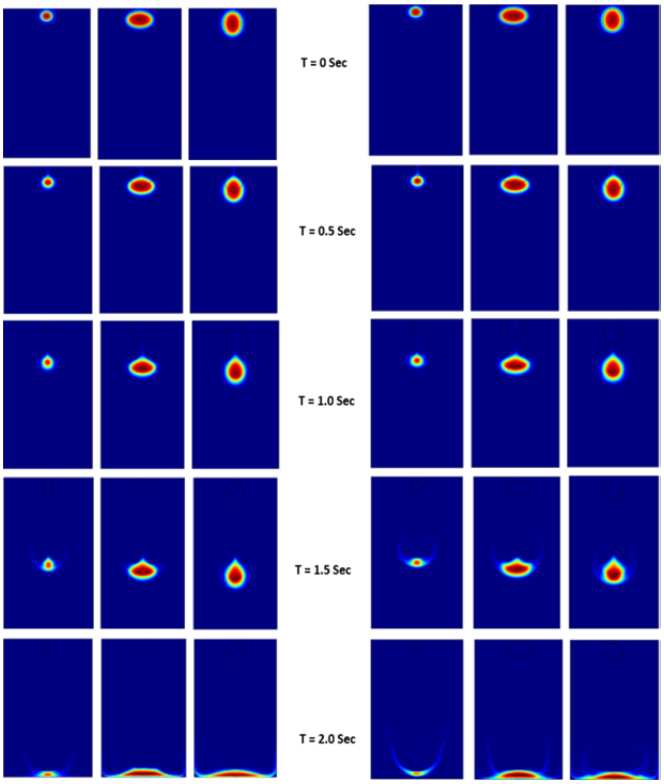

Fig. 3 Volume fraction contours of spherical and spheroidal Carreau model fluid droplets of n-0.4 settling in stagnant air a) Spherical b) Oblate ellipsoid c) prolate ellipsoid

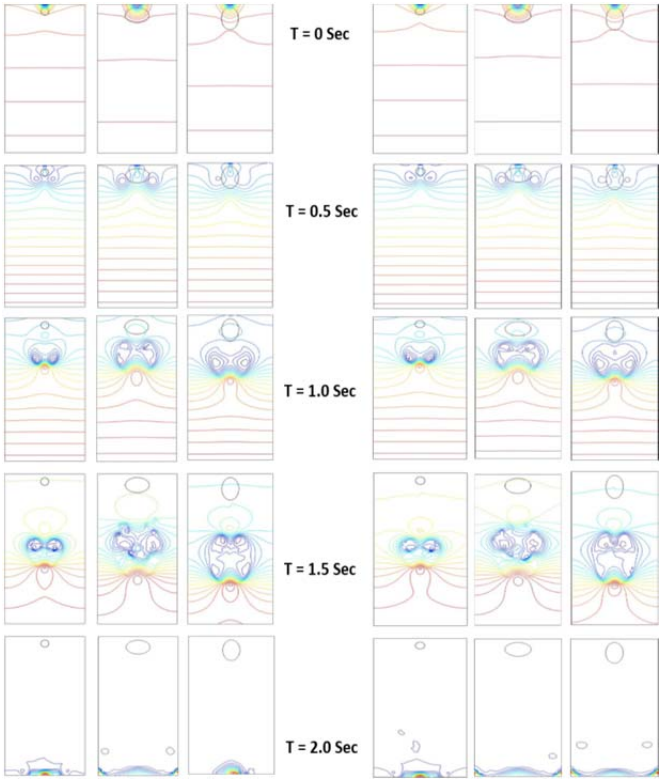

Fig. 4 Pressure Distribution of spherical and spheroidal Carreau model fluid droplets of n-0.4 settling in stagnant air a) Spherical b) Oblate ellipsoid c) prolate ellipsoid

The internal recirculation phenomenon seen in Fig. 4 can be explained as follows: if the boundary of an air flow is solid, the no slip boundary condition states that air is in contact with a relatively at rest boundary. In the case of non-Newtonian drops falling in a continuous stagnant medium of air, it is observed that the drops of viscous liquids resist breakup due to the resistance of developing internal recirculation's, and an increase in viscosity plays an important role in suppressing drop breakup by inhibiting rapid internal motions. In the case of oversize drops, however, this phenomenon is reversed. The pressure coefficients for the spheres gradually decrease in flow fields where viscosity is a major factor. Thus, the trend of the pressure distribution at various time steps seems to be similar for all the cases of Non-Newtonian droplets.

4.4 Velocity field streamlines

Streamlines are tangential to the flow's velocity vector, which represents the fluid element's direction at any point in time. When a droplet falls freely due to gravity, the pressure gradient at the top surface of the droplet is greater. As time passes, the domain fluid penetrates the droplet, causing the bottom surface to approach the droplet cap. Along with this, the droplet velocity increases normally until it reaches a nearly stable value and then decreases when it hits the bottom of the wall. As the velocity of a freely settling droplet increases, the shape of the droplet changes from spherical to shell. The velocity distribution around a free-falling droplet in which the droplet pushes the liquid downward and a toroidal vortex forms on the droplet's side. The significant velocity gradients in front of the droplet are depicted in the flow field. As time passes, the velocity difference decreases and approaches a constant value, which can be considered the droplet's terminal velocity. In this study, no specific velocity is given for the droplet to move because it is falling freely due to gravity forces, and thus there is no recirculation. The velocity distributions around the Power-law and Carreau model droplets freely settling in the stagnant air medium are shown in Fig. 5. The velocity distributions for prolate and oblate shaped droplets are found to be closely related to the Carreau and power law systems. The falling drop pushes the liquid downwards and in front of it, and the liquid flows back into the bubble wake, forming the vortex at the drop's fore–aft symmetry. When the velocity of the falling droplet increases, the convection forces increase in comparison to the viscous forces. The recirculation trend will vary with the dilatational behavior of the fluids, as shown in Figure 5. When a water drop falls freely with a constant velocity, it is expected to oscillate with periodic vortex shedding in the unstable wake. This is known as the terminal velocity. Such drop oscillations will tend to disrupt the drop's regular steady internal recirculation, reducing overall internal recirculation. However, as the shear thinning effects increase, so does the vortex. The higher the interfacial tension, the faster the ring will form, as illustrated in Figure 5. The flow field exhibits a significant velocity gradient in front of the drop, which corresponds to the high shear rate region at the front. Second, the presence of walls may suppress the convection force, but the wall effects are ignored in the current study. The retardation effects of the wall are reduced as a result of the wall's unconfinement, and a small recirculation is observed. When the velocity of the falling droplet increases, the convection forces increase in comparison to the viscous forces. The size of the vo rtex created by the Newtonian fluid is greater for non-Newtonian and power-law droplets than for shear thinning fluids, and as the value of 'n' decreases, the size of the vortex becomes smaller, so reverse flow is small for shear thinning fluids. This demonstrates that the length of the recirculation is inversely proportional to the power law index, wall factor, and Reynolds number.

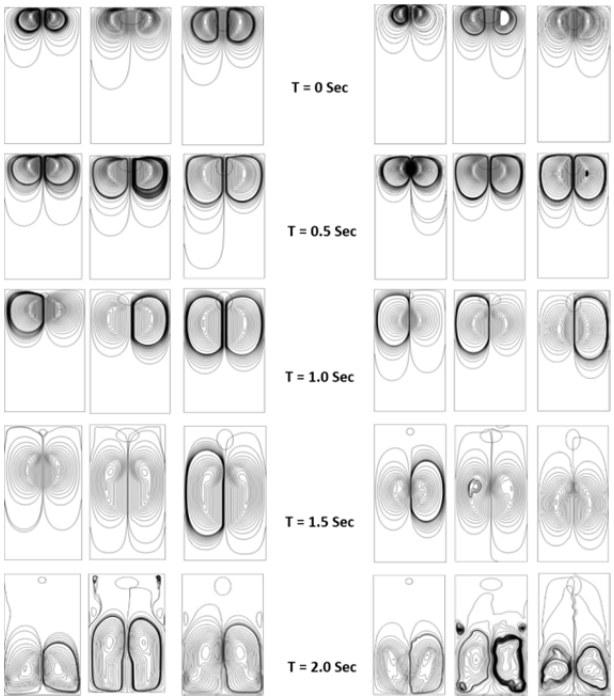

Fig. 5 Velocity Distribution of spherical and spheroidal Carreau model fluid droplets of n-0.4 settling in stagnant air a) Spherical b) Oblate ellipsoid c) prolate ellipsoid

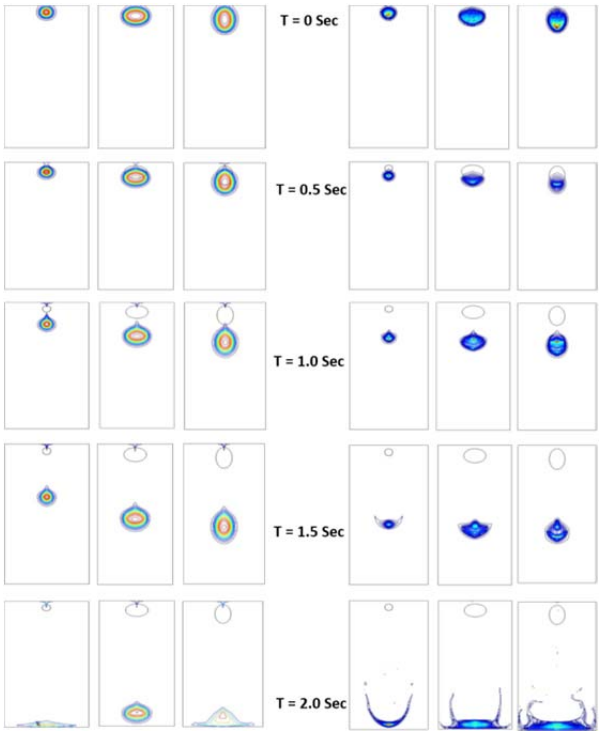

Fig. 6 Viscosity Distribution of spherical and spheroidal Carreau model fluid droplets of n-0.4 settling in stagnant air a) Spherical b) Oblate ellipsoid c) prolate ellipsoid

4.5 Viscosity Distribution

If the viscosity of the suspension is larger than the viscosity of the suspending fluid at low shear rates, the droplets remain spherical because of the surface tension (Funfschilling, 2006). When the shear rate is high enough to distort the bubbles sufficiently and diminish the mixture's viscosity. The complicated rheological behavior of non-Newtonian fluids makes the viscosity vulnerable to shear stress as well. A non-Newtonian fluid's viscosity near a rising droplet is considerably different from the local viscosity near a falling droplet because of the relative motion of the fluids. Therefore, it is essential to know the local viscosity distribution around the rising or falling droplet in non-Newtonian fluids in order to explain droplet movement. Newtonian (stagnant air). For the Carreau model system and the power law droplets, the droplet's shape and motion are significantly different at t=0.5 seconds. An oblate spheroid bubble forms as the shear thinning intensifies. The viscosity of shear thinning fluids changes as the shear rate increases, and this change is linked to the magnitude of the velocity vector indirectly. Viscosity with an infinite shear rate increases in the downstream direction as speed rises. Additionally, lower viscosity affects the drop motion. When compared to the Emkarox droplet, the Carreau model's trend is substantially different, showing that the dispersed phase's shear thinning impact is greater and the droplet's zero shear rate viscosity is extremely high (Fig. 6). The shear thinning effect in non-Newtonian fluids is caused by the non-uniformity of the liquid flow around the moving and deforming drop. As a result, viscosity variations have a major impact on the drop forms and deformations in the case of the power-law droplet. Because of this, when a drop is deformed or moved, the shear thinning effect is greatly increased due to low viscosity, which in turn increases deformation.

5. CONCLUSIONS

In this study, many features of falling droplet movement, such as the droplet's shape while falling, the droplet's terminal velocity are calculated. Different droplet forms and velocities at different time intervals are studied numerically. Droplets of various forms and velocities are studied numerically at time intervals ranging from 0 to 2 seconds. To put it another way: The surrounding liquid's viscous forces influence drop deformation, together with external perturbations caused by wall effects and dimensionless characteristics such as Reynolds number, Weber number and Bond number. From the velocity distribution contours, it can be seen that the velocity steadily increases as it falls freely and achieves nearly constant values before hitting the bottom of the channel's walls. In the simulation, the droplet does not move due to the absence of an entrance velocity. Variations in fluid parameters, such as viscosity and deformation, appear to be almost equal in terms of velocity variation. In the case of drop deformation and motion, the viscous effects are quite significant, and the shear thinning impact is particularly large when the viscosity is low, which amplifies the deformation.

REFERENCES

Acharya, A., Mashelkar, R. A., & Ulbrecht, J. (1977). "Mechanics of bubble motion and deformation in non-Newtonian media." *Chemical Engineering Science*, **32**(8), 863-872.

Acharya, A., Mashelkar, R. A., & Ulbrecht, J. (1978). "Motion of liquid drops in rheologically complex fluids." *The Canadian Journal of Chemical Engineering*, **56**(1), 19-25.

Bird, R.B., Stewart, W.E. & Lightfoot, E.N. (1960). *Transport Phenomena. Wiley Publications, New York.*

Chhabra, R. P. (2006). *Bubbles, drops, and particles in non-Newtonian fluids*. CRC press.

Chhabra, R.P. & Richardson, J.F. (2008). *Non-Newtonian flow and applied rheology, Second Edition. Oxford Publications*.

Clift, R. Grace, J.R., Weber, M.E. (1978). *Bubbles Drops and Particles. Academic Press. New York.*

Coutanceau, M., & Thizon, P. (1981). "Wall effect on the bubble behaviour in highly viscous liquids." *Journal of Fluid Mechanics*, *107*, 339-373.

Dong, H., Wang, X., Liu, L., Zhang, X., & Zhang, S. (2010). "The rise and deformation of a single bubble in ionic liquids." *Chemical Engineering Science*, **65**(10), 3240-3248.

Funfschilling, D., & Li, H. Z. (2006). "Effects of the injection period on the rise velocity and shape of a bubble in a non-Newtonian fluid." *Chemical Engineering Research and Design*, **84**(10), 875-883.

Garner, F. H., & Hammerton, D. (1954). "Circulation inside gas bubbles." *Chemical Engineering Science*, **3**(1), 1-11.

Gollakota, A. R., & Kishore, N. (2018). "CFD study on rise and deformation characteristics of buoyancy-driven spheroid bubbles in stagnant Carreau model non-Newtonian fluids." *Theoretical and Computational Fluid Dynamics*, **32**(1), 35-46.

Ismail, M. (2007). "Level-Set and phase field methods: Application to moving interfaces and two-phase fluid flows". *Scientific computing.*

Kennedy, M. R., Pozrikidis, C., & Skalak, R. (1994). "Motion and deformation of liquid drops, and the rheology of dilute emulsions in simple shear flow." *Computers & fluids*, **23**(2), 251-278.

Mohan, V., Nagarajan, R., & Venkateswarlu, D. (1972). "Fall of drops in non-newtonian media." *The Canadian Journal of Chemical Engineering*, **50**(1), 37-40.

Rust, A. C., & Manga, M. (2002). "Effects of bubble deformation on the viscosity of dilute suspensions." *Journal of non-newtonian fluid mechanics*, **104**(1), 53-63.

Spilhaus, A. F. (1948). "Raindrop size, shape and falling speed." *Journal of the Atmospheric Sciences*, **5**(3), 108-110.

Taylor, T. D., & Acrivos, A. (1964). "On the deformation and drag of a falling viscous drop at low Reynolds number." *Journal of Fluid Mechanics*, **18**(3), 466-476.

Zhang, L., Yang, C., & Mao, Z. S. (2010). "Numerical simulation of a bubble rising in shear-thinning fluids." *Journal of Non-Newtonian Fluid Mechanics*, **165**(11-12), 555-567.